

Power-optimized symmetrizing current control with a 8.7 kNm-Transverse Flux Generator

Jochen Schüttler, Holger Groke, Marek Siatkowski, Johannes Adler, Bernd Orlik
Institute for Electrical Drives, Power Electronics and Devices (IALB), University of Bremen
JSchuettler@ialb.uni-bremen.de

Abstract-Transverse flux machines (TFM) have been proposed as a powerful direct drive alternative. The construction and control of TFM have often proved a problem. In this paper the construction of a working transverse flux generator is presented. Its characteristics are predicted by a detailed FE simulation. Also a current control is designed that compensates unsymmetries and maximizes the power output. Measurements finish this work.

I. INTRODUCTION

Applications for electrical drives often call for high torque at low speed, and with a compact device. Especially in wind energy scenarios the need for such a drive is obvious; rotor speed is low, torque is high, and the housing and shaft of a windmill are strongly dependent on the size of the drive. But with classical ac or dc drives this cannot be done without a gear box or large engine diameters and lengths.

Transverse flux machines (TFM) have been proposed for just this kind of scenario, their typical huge advantage is their extremely high force density, besides lower energy

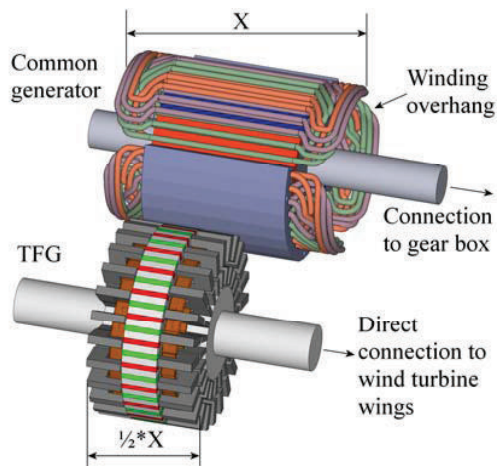


Fig. 1. Conventional rotor and TFG rotor, comparison in length losses due to the absence of any winding overhang (Fig. 1).

The construction of real TFM has often proved to be a fickle job with many obstacles. But at IALB & LDW (Lloyd Dynamowerke GmbH), Bremen, Germany, such a water-cooled machine was built, at a torque of 8.7 kNm. It is meant as a small scale test model for a later 1 MVA transverse flux generator (TFG), planned as an EU facilitated project led by BCM (Bremen Center of Mechatronics).

As will be shown, TFM feature a generally high stator leakage inductance, resulting in a low power factor as a disadvantage [5]. In generator applications a power factor



Fig. 2. The TFG designed and built by IALB / LDW

correction (PFC) is essential to optimize the energy output, here done by an active, frequency converter driven load. The converter is already a must for grid power injection. In this case, the converter was built as part of the project.

Secondly these machines show high non-sinusoidal cogging torque. Thirdly they tend to suffer from unsymmetrical phases. Both call for correcting current shaping. This paper addresses symmetrizing currents only, a torque smoothing algorithm [6] will be applied later on.

So TFG behavior optimizing control is addressed, the second main challenge in utilizing this strongly advantageous machine type. Measurements show the control results.

II. TRANSVERSE FLUX PRINCIPLE

The typical feature of TFM is the magnetic flux path which has sections where the flux is transverse to the rotation plane. Another distinctive feature is the ring-shaped winding in the stator in which the direction of the current corresponds with the movement direction of the rotor. The design of the flux path combined with the use of new magnet materials lead to very high-performance machines with three to five times higher power densities compared to conventional dc, synchronous or induction machines. This means a transverse flux machine with the same power rating is reduced in size and weight compared to conventional machines. An additional advantage of transverse flux machines is their higher efficiency. There are two main reasons for this: the reduced copper losses, due to the absence of winding overhang in stator winding, and the fact that the magnetic circuit and the electrical circuit don't share the same space.

The principle allows for a lot of very different design variants: Inner, middle or outer rotor, claw pole design, skewed poles, skewed magnets, turns per coil and phase, number of airgaps per phase, etc. Typically only three major topologies need to be discerned: Pure reluctance machines (TFRM) or permanent magnet excited layouts (TFPM), which can be divided into flat magnet (Fig. 3) and flux concentrating layout (Fig. 4).

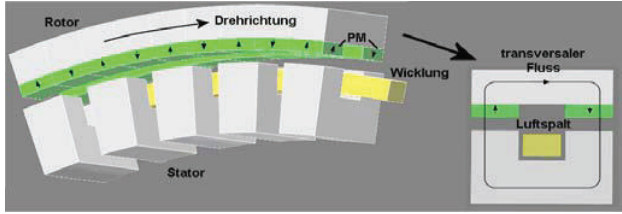


Fig. 3. Flat magnet TFPM layout, transverse flux plane

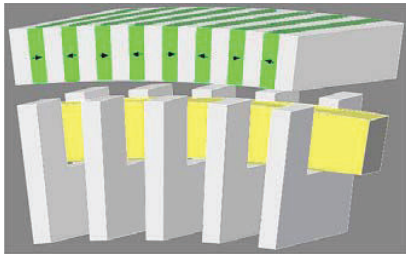


Fig. 4. Flux concentrating TFPM layout

The reluctance machine has the least force density and needs more phases to work. Still the absence of permanent magnets may offer an advantage in material and construction costs. The transverse flux motor in flux concentrating configuration can achieve high force density but has a higher amplitude of torque ripples. The flat magnet configuration has a middle-high force density, but depending on the surface mounted magnets, less torque ripples than the flux concentrating topology. It is also easier to construct.

At present, the force densities of normal asynchronous motors can achieve up to 20-30 kN/m². Water-cooled and force density optimized high-performance machines can reach 65 kN/m² and for a short time even up to 80 kN/m². The norm for the synchronous machines complies with 40-60 kN/m². Transverse flux reluctance machines can achieve up to 60 kN/m² and the water-cooled permanent magnet transverse flux machine yields more than 200 kN/m² [1].

Besides the described advantages there are a few disadvantages of transverse flux machines. These are the before-said ripples in the torque shape, the normal force fluctuation, the low power factor and the complex core design (especially for flux-concentrating layout). The torque ripples and normal force fluctuation produce noise and vibrations. There are some kinds of solutions to reduce the torque ripples and the normal force fluctuation. One of them is modifying the geometry for the magnetic path [3]. Furthermore, an appropriate current wave form can be applied to the machine [2],[4].

III. DESIGN OF THE GENERATOR SYSTEM

A. 8.7 kNm-Transverse Flux Generator (LDW)

For optimal performance a water-cooled, flux concentrating variant was designed. The compact build we aimed for let us choose a 4-phase layout. Each phase has two coils left and right of the rotor discs (fig. 5,6).

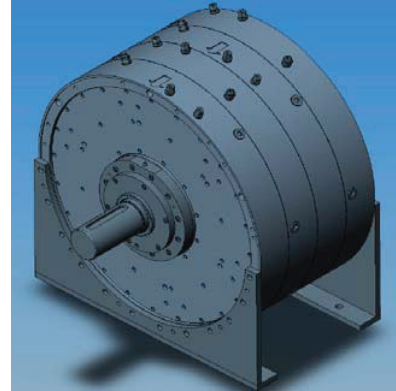


Fig. 5. Full view of the TFG

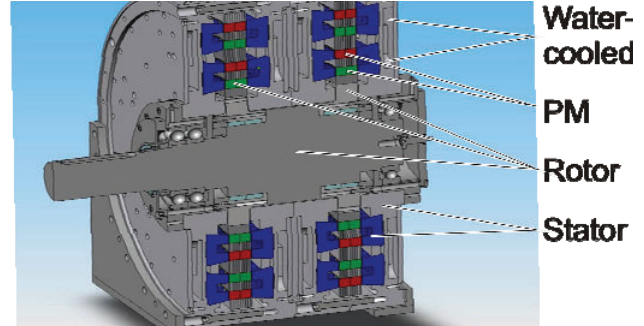


Fig. 6. Section view of the TFG

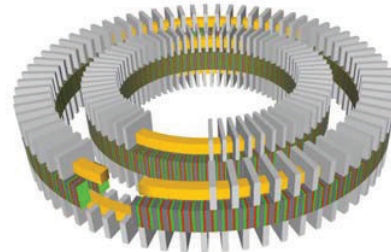


Fig. 7. Magnetomechanical active parts of two phases on one disk

Both rotor discs hold two phases, which are in sync to each other (fig. 7). As they have different amounts of PM material the magnitude of their electrical quantities differs. Also the rotor discs are displaced by $\pi/2$ to each other, which allows for four different, ac driven electrical phases.

The two synchronized phases could be interconnected in series or parallel. But with a series connection high-voltage power devices of more than 1000 V would be needed, where a parallel layout would result in unwanted current distributions, if the induced voltages of both phases are not perfectly equal. So a frequency converter for four phases was designed, which will be described in the following chapter.

B. Frequency Converter & Controller Board

By use of Convertteam LV7000 power converters a 4 phase converter was designed and built. It features a TI-controller board that is programmed, parametrized and monitored by an IPC with RS232 or USB-interface (fig. 8). The controller board manages phase-angle adjusted power feedback from the dc link into the supply grid. This will not be discussed in further detail.

Secondly the controller board preprocesses the encoder signals to get the rotor position angle ϵ , and calculates a power control generated reference value for the torque t_{ref} . Both are sent to four sub-controller boards that achieve this reference torque, feeding power into the dc link.

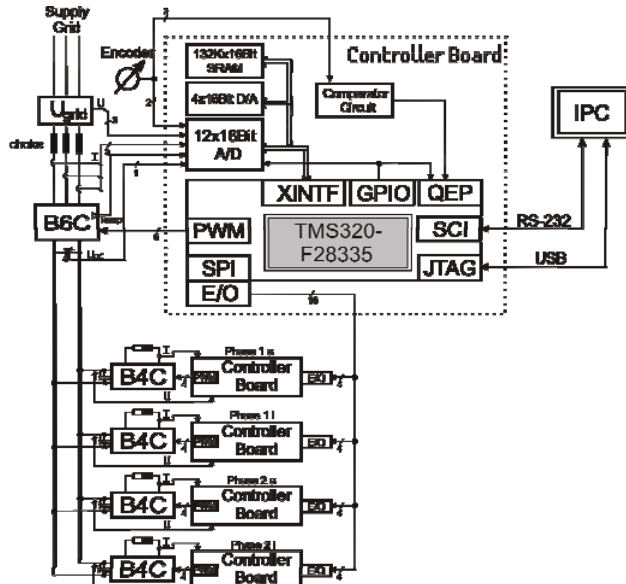


Fig. 8. Full diagram of power and signal lines

Fig. 9 shows the switchgear cabinet holding all described parts. The five converter units are connected by the left-side dc-link. The middle converter is the master station, both upper and lower units are slaves. Each unit features its own controller board (Fig. 10), which are connected by high-capacity optical fibres (Fig. 11).



Fig. 9. Switchgear cabinet, with master station (blue) and four slaves (red)

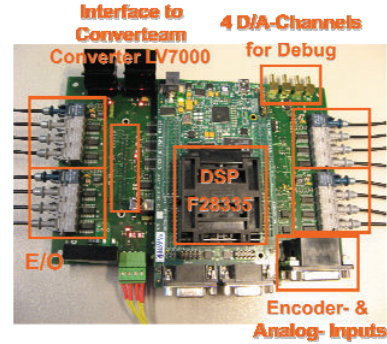


Fig. 10. Controller board with sub-group highlighting

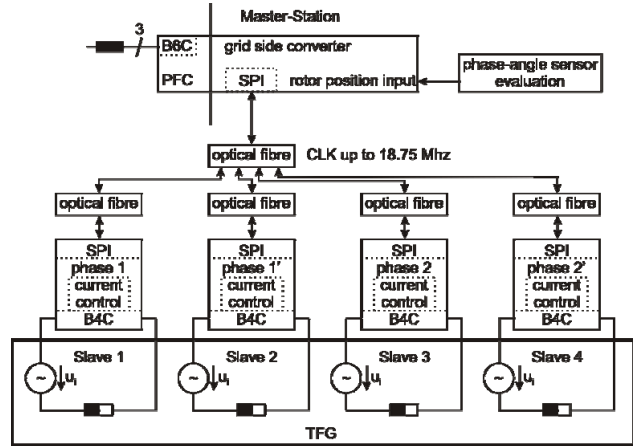


Fig. 11. optical fibre connection between master and slaves

IV. SIMULATION OF THE TFG

In the planning stage of the TFG design a 3D FE simulation was developed that helped in choosing the geometry form and parameters. In Fig. 12 the final geometry is shown with the applied FE mesh for solution. Only one double pole pitch needs to be simulated with the assumption of perfect symmetry.

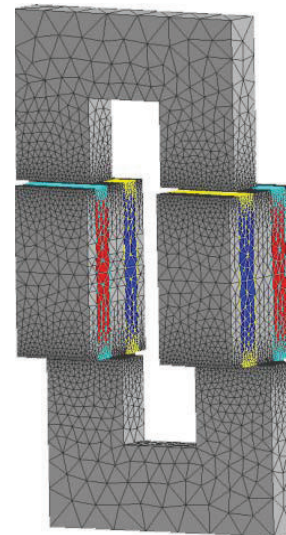


Fig. 12. Mesh of the TFG FE simulation

Fig. 13 shows the geometry with color shading as indication for the calculated magnetic induction at specific operating points concerning the electrical current and the rotor position.

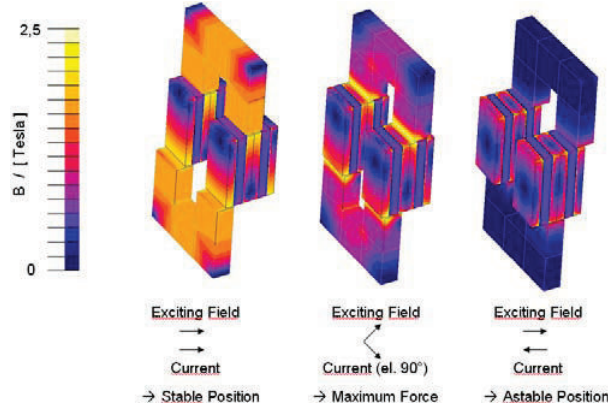


Fig. 13. Simulated magnetic induction, shown as color shades

In later stages it became also important in generating reference curves for control scenarios. Fig. 14 shows the simulated induced voltages for the four phases.

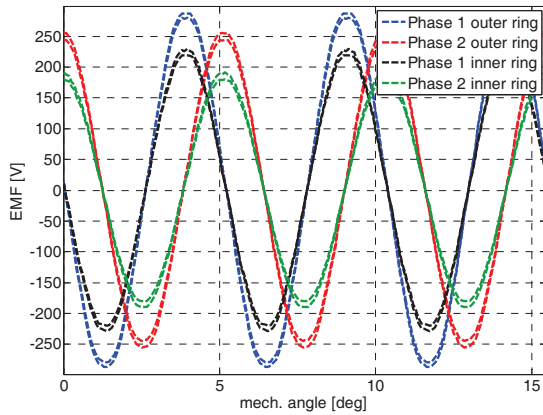


Fig. 14. Simulated induced voltages for all four phases

The simulation needs about one week to run for each phase, or even longer if eddy current losses are taken into account. A new method to significantly improve the simulation time will be presented in the near future.

V. CONTROL OF THE TFG

A principle disadvantage of TFM is their low power factor due to their high stator leakage inductance. It leads to a strong current phase displacement when loaded with a small resistor or short-cut (cf. *Measurements*). This results in a high reactive power but small real power output. Also a technical problem results: The peak current occurs simultaneously with the overlapping of stator and rotor poles. Only a small torque results, which is in accordance to the small power output. But the high normal force on the rotor is increased, leading to destructive oscillating forces.

Secondly it's almost impossible to set up exactly equal air gaps for each phase, so their electrical behaviour differs slightly (cf. *Measurements*). To symmetrize the phases and accomplish the needed power factor correction an active current control is needed for each phase. The converter set-up is prepared for this control by use of a DSP controller board for each phase converter (cf. *Design*).

If there was no leakage inductance the power factor would be optimal. The induced voltage would drive only a resistive load, resulting in a cophasal current of the same shape. So the main idea for this control is the use of a normalized, measured open-circuit voltage as a current reference signal.

The master station provides the preprocessed rotor angle ε_{meas} and a power optimizing torque reference value t_{ref} for each phase, transmitted by optical fibre (LWL). The measured phase current I_{meas} is provided by A/D-conversion. The rotor angle is used as base for the normalized reference current shape $I_{ref,0}$. This is multiplied with the torque reference t_{ref} , resulting in the optimized cophasal reference current I_{ref} . This will be impressed by a standard PI-controller, also using the injected voltage as a disturbance feedforward control signal u_{dist} . This is gained by multiplying the rotor angle dependent normalized induced voltage shape $u_{i,0}$ with the rotor speed ω . The

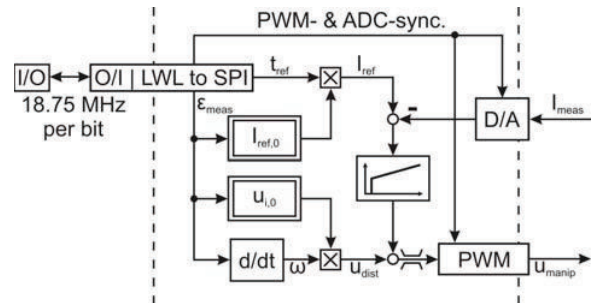


Fig. 15. The control structure for each TFG phase

resulting value is limited to the dc-link voltage and given to a PWM generator, thus driving the TFG phase with the manipulating voltage u_{manip} . PWM and ADC are synchronized to the master station input. The overall control structure is shown in Fig. 15.

VI. MEASUREMENTS

In order to verify the FE model predictions and get the induced voltage curves needed for the control we measured the no-load voltage of each coil. The results are shown in Fig. 16. The before-said small unsymmetries can be seen clearly.

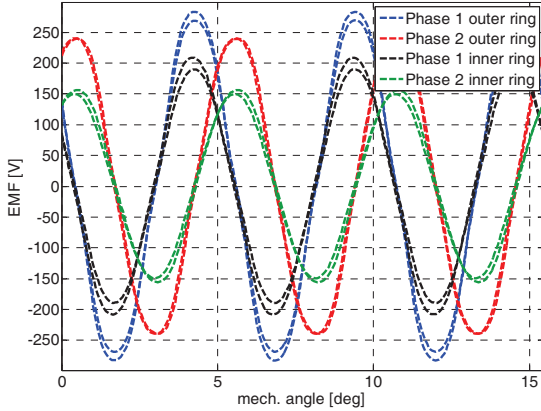


Fig. 16. Measured no-load voltages of the coils at 55 rpm

Comparison with the FE *simulation* results show fairly good accordance, especially with the outer rings. Remaining differences result from changes in the air gap width over the circumference.

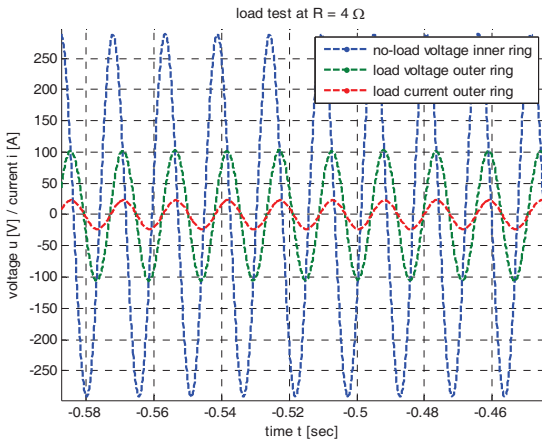


Fig. 17. Measured currents and voltages at an ohmic load of 4 Ω

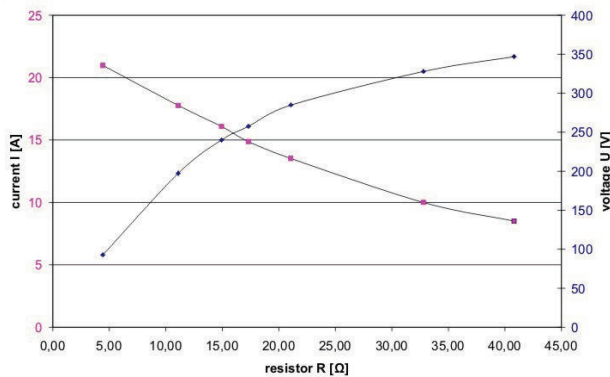


Fig. 18. Current (magenta) / voltage (dark blue) rms values over ohmic load

When the induced voltage is loaded with a small resistor the resulting currents are very low, due to the low power factor (Fig. 17 & fig. 18). With the power converter active load, but without any control, similar currents occur. In Fig. 19 the yellow curve is the phase current, the green curve is the measured no-load voltage of the second coil from the same phase, the light blue curve is a relative curve of the reference current, cophasal with the no-load voltage. Additionally the magenta curve is the current of the second phase. It shows the current phase-lag to be about $\pi/3$ and the unsymmetry between the phases. Also the current waveform is not the same as the reference curve.

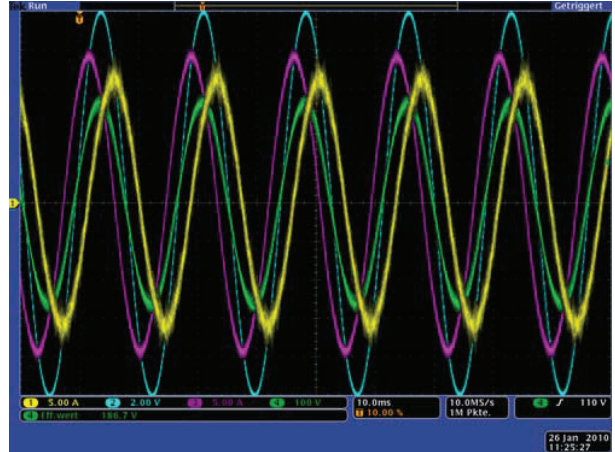


Fig. 19. Currents and no-load voltage without current control

With the current control activated and parametrized correctly the curves in Fig. 20 are a measured result. They show the same as before, without the second phase current. Now the current shape matches the no-load voltage and is perfectly in phase, resulting in a power factor of one.

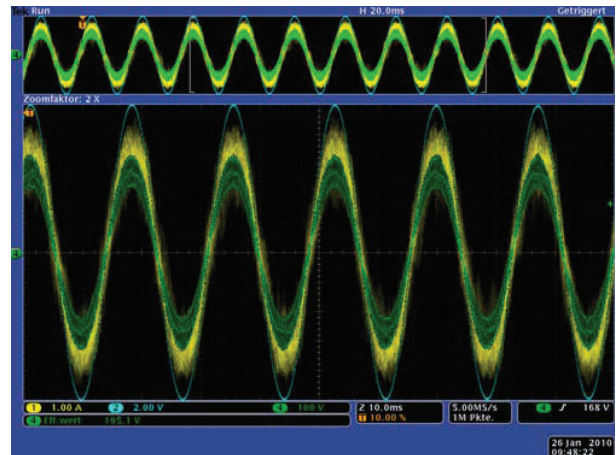


Fig. 20. Current and no-load voltage with current control

The current probe shows a strong disturbance noise. Better measure results can be found by programming the microcontroller board to show the A/D-converted currents as D/A-output signals. All four phase currents are shown in Fig. 21, cophasal and mostly symmetric. The proportional factor is 12.8 A/V.



Fig. 21. Currents of both inner and outer phases

VII. CONCLUSION

A transverse flux generator with a torque of 8.7 kNm was designed, simulated and constructed. Also a microcontroller DSP-Board was developed, that is able to control a four phase converter for grid power feedback. In test runs we were able to imprint currents that symmetrize the TFG phases and optimize the power output by an active power factor compensation. As a remaining task torque smoothing current waveforms will be calculated that minimize vibration and oscillating stress inside the machine while keeping the improvements gained so far. All of this is a working small-scaled case study for a 1 MW wind energy TFG that can significantly increase economical and, as a consequence, ecological advantages.

ACKNOWLEDGMENT

We thank the BCM for its continuing support during concerning projects. We thank LDW for their long-year partnership in building several TFM prototypes. We thank Convertteam, Atlas Magnetics, Centiv and Tritecc for their cooperation in the current EU project.

REFERENCES

- [1] H. Weh, H. May: "Achievable force densities for permanent magnet excited machines in new configurations", ICEM Munich, Germany, 1986
- [2] J. Schüttler: "Regelung von Transversalflussmaschinen", IALB, University of Bremen, Germany, 2004 (unpublished)
- [3] M. Vinogradski, U. Werner, B. Orlik: "Genetic Algorithms Used for Geometrical Structure Design of Transverse Flux Permanent Magnet Motors to Optimize the Torque Wave Form", PCIM Nürnberg, Germany, 2004
- [4] U. Werner, H. Raffel, O. Harling, N. Parspour, B. Orlik: "Strategies to Reduce Torque and Current Ripples of Transverse Flux Permanent Magnet Generators for Wind Turbine Applications", EPE Toulouse, France, 2003
- [5] D. Svehkarenko, J. Soulard, C. Sadarangani: „A Novel Transverse Flux Generator in Direct-Driven Wind Turbines“, ICEM Chania, Greece, 2006
- [6] U. Werner, J. Schüttler, B. Orlik: „Position control of a Transverse Flux Motor with reduced torque ripples for Direct Servo-Drive Applications using shaped currents with harmonics control“, EPE Aalborg, Denmark, 2007